

Aviation emission, contrail length, and flight level determination for en-route flight path decision

Kam K.H. Ng ^{a,*}, C. W. Yu ^a, T. W. Lam ^a, K. K. L. Cheung ^a

^a*Department of Aeronautical and Aviation Engineering, The Hong Kong Polytechnic University, Hong Kong SAR, China*

* *Corresponding author.*

Email Address: kam.kh.ng@polyu.edu.hk (Kam K.H. Ng), savio.cw.yu@connect.polyu.hk (C. W. Yu), kevin.tw.lam@connect.polyu.hk (T. W. Lam), loklarry.cheung@connect.polyu.hk (K. K. L. Cheung).

Acknowledgment

The research is supported by *Department of Aeronautical and Aviation Engineering, The Hong Kong Polytechnic University, Hong Kong SAR*. Our gratitude is also extended to the Research Committee of the *Department of Aeronautical and Aviation Engineering, The Hong Kong Polytechnic University* for support of the project (UALL).

Declarations of interest: The authors declare that they have no known competing financial interests or personal relationships that could have appeared to influence the work reported in this paper.

Aviation emission, contrail length, and flight level determination for en-route flight path decision

Abstract

The rapid growth of the aviation industry and air travel brought along increased air traffic in the airspace, greater fuel consumption, and more engine emissions. It is estimated that the aviation sector contributes roughly 4.9% of total radiative forcing in Earth's atmosphere in 2005, with the CO₂ and NO emissions expected to rise by a factor of 2.0-3.6 and 1.2-2.7 respectively by 2050 [1]. While the industry is actively trying to mitigate carbon and nitrogen emissions through the introduction of alternative jet fuel and higher efficiency engines, the issue remains that contrails and cirrus clouds created by aircraft emissions in the upper troposphere and lower stratosphere remain as the one of the main contributors to climate change. Estimation in 2005 concluded that contrails contributes approximately 6-15 mW m⁻² and cirrus clouds contributes between 10-80 mW m⁻² towards global radiative forcing [2]. In order to help alleviate climate change, it is proposed with flight path optimization, aircrafts will be able to avoid areas where contrail formations will be the most likely, thus reducing the amount of cirrus clouds within the UT/LS layer.

The aim of this project is to develop an air traffic flow model with the intentions of reducing contrail formations and other aviation emissions as the main objective. Using the China South Airlines Urumqi to Shanghai flight route as the main studying sample, atmospheric data from en-route cities will be taken and compared with pre-established contrail formation parameters. An air traffic flow model will then be created using the parameters and variables obtained, thus establishing a comprehensive system in assisting the pilots in making the decision of switching flight level in order to avoid the contrail zones.

Keywords: Air traffic flow decision, flight levels, mitigation strategy, aviation emission

1. Introduction

1.1. Introduction

The aviation industry is growing at a fast and steady pace, with the number of airline flights around the world increasing by 70% during 2004 to 2019 [3]. The increasing flights, and subsequently the number of aircrafts in the air, resulted in greater fuel consumption and more engine emissions [1]. Typically, aircraft emissions include carbon dioxide, nitrogen oxides, contrails, and aerosols containing sulphurs and soot. The increase in the number of flights is predicted to cause a rise in the amount greenhouse gases emitted, with the sector estimated to take up around 12% of total CO₂ emission from transportation globally in 2050 [1]. The predicted increase in air traffic will also result in the rise of contrail formations in the atmosphere, and while the impact of contrails and aviation-induced cirrus clouds on global climate change is not yet fully understood by the scientific community, it is certain that their contribution towards the global radiation budget and climate forcing will increase proportionally.

The start of the jet age in the 1950s changed the ways of air travel, with planes flying higher and faster over longer distances. Despite the long history of air travel and the introduction of the jet engine, the effects of them on the global environment were not explored until the 1970s, with concerns over the possible ozone depletion, atmospheric infrared and solar radiation scattering within and above the contrail sheets caused by supersonic aircrafts flying in the stratosphere [4]. Investigations on the effects of subsonic aircrafts emissions in the troposphere only started in late 1980s, with national organizations such as NASA and European Commission DG XII starting the Subsonic Assessment SASS and AERONOX [5, 6] project respectively, aiming to better understand the effects of nitrogen oxide emissions on the formation of ozone and contrails. This also marks the first-time aviation atmospheric impact assessment switched from landing and take-off phase to cruising phase where the aircraft spends most of the time in. The shift in research focus is due to the characteristics of the boundary layer between the upper troposphere and lower stratosphere. Air in that location is relatively still and lacks any sufficient means of scrubbing away any unwanted particles and gas such as carbon dioxide. Aircrafts operating in that region will directly emit any materials into the layer, resulting in a build-up of emission particles and gases [5]. The location of the emission will also increase their effectiveness in causing chemical and aerosol reaction, such as isobaric cloud formation and ozone generation, which will contribute to climate change.

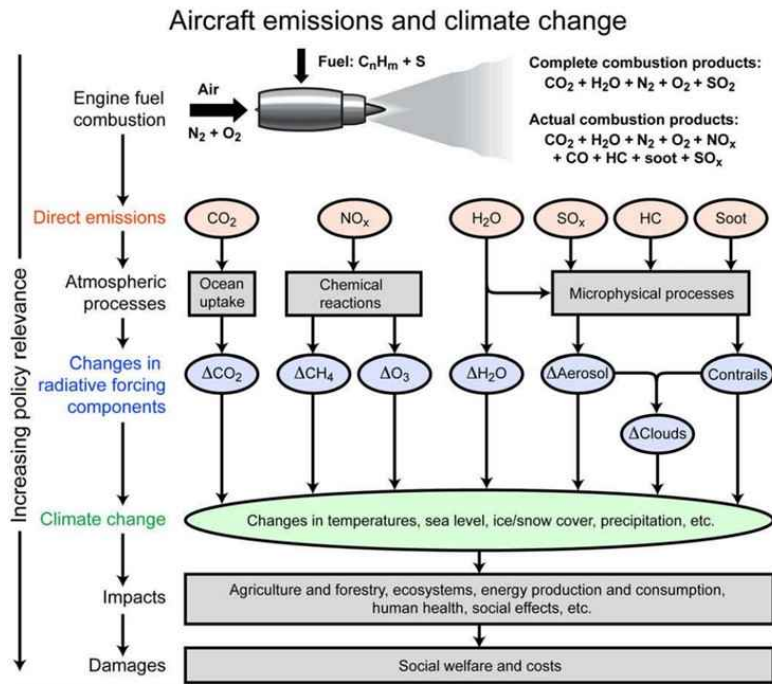


Figure 1. Typical aircraft emissions and impacts towards climate change. [7]

While an aircraft's turbine engine operates similarly to normal internal combustion engines, with almost identical exhaust emissions, the effects of the emission substances affects the global climate differently when comparing to the greenhouse gases that are emitted at ground level. At higher levels, the effects of contrail and other aircraft emissions on global climate is quantify on their respective radiative forcing. According to Lee[7], the contribution towards global radiative forcing of aircraft emissions can be classified as the following:

- CO₂ emission → +RF
- NO_x emission → +RF
- H₂O emission → +RF
- Linear contrail formations → +RF
- Aviation-induced cirrus clouds → +RF
- Sulphate particles emission → -RF
- Soot particles emission → +RF

The formations of contrail and cirrus clouds are directly linked to the amount of soot particles emitted by the engines, as well as other environmental factors, such as ambient temperature, ice and water saturation, and air pressure. As aircraft enters a sufficiently cold airstream, the hotter and humid exhaust plume will mix with ambient air and form contrails behind the aircraft. As temperature increases, ice saturation ration within the contrail with increase, while larger aerosol radii size will support a lower ice saturation ratio[8]. Ambient air pressure will affect the isobaric mixing of hot exhaust and cold atmospheric air, and by comparing with the baseline Schmidt-Appleman criterion and ambient water vapour saturation pressure, we will be able to

determine if the exhaust plume is sufficient for droplet formation, and thus contrail generation [9].

Currently, within the aviation industry, there are multiple ongoing projects for promoting sustainability concerning the atmosphere and climate change, namely noise reduction, air quality improvements, biofuel/alternative fuel usage, and aircrafts efficiency increase.

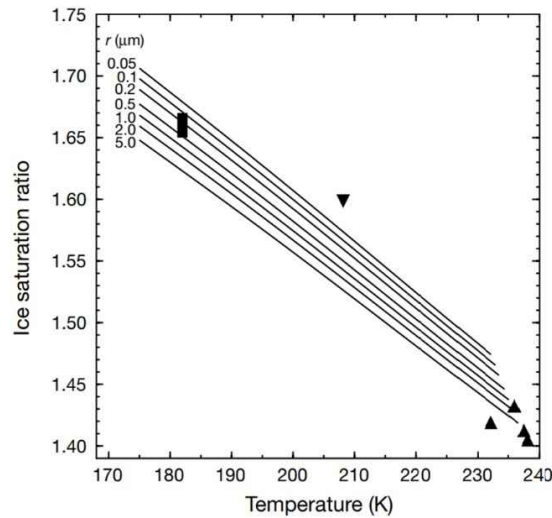


Figure 2. Contrail ice saturation ratio for various aerosol radii, comparing to ambient temperature. [8]

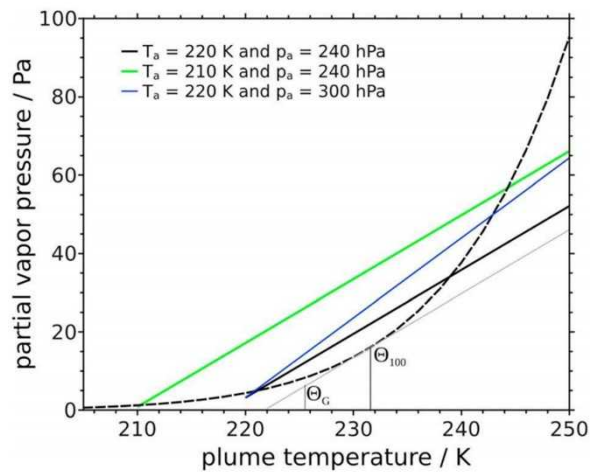


Figure 3. Contrail ice saturation ratio for various aerosol radii, comparing to ambient temperature. [8]

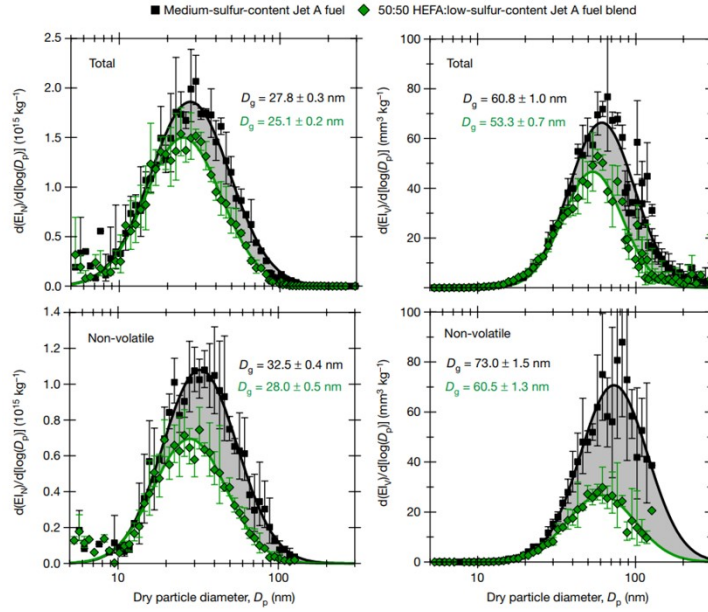


Figure 4. Emitted particle size at high thrust cruise condition for conventional Jet A fuel and 50:50 HEFA: low sulphur Jet A fuel blend comparison. [10]

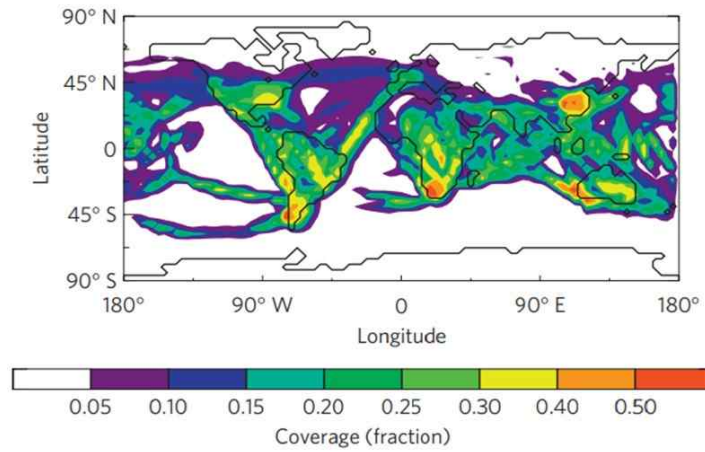


Figure 5. Global cirrus cloud coverage caused by young contrails (age less than 5 hours). [2]

While most are still in the experimental stages, the most feasible method for combating climate change will be managing the emissions of aircrafts. The use of alternative fuel has proven to be useful in reducing the amount of greenhouse gases such as carbon dioxide and nitrogen oxides. Taking the emission data from the burning of a 50:50 Hydrotreated esters and fatty acids (HEFA): low-sulphur Jet A, the reduction in carbon dioxide and nitrogen oxides is apparent. However, Moore et. al. [10] reported that the amount of soot particles “remains in the soot-rich regime (around 10^{14} kg^{-1})”, besides, the 8% increase in hydrogen content compared to conventional Jet A fuel also raises concern of higher chance of contrail formation and higher ice content. At the same time, contrail formation control remains the most effective and easier to implement comparing to the other methods for promoting sustainability. The better developed protocols and system for air flow traffic management can also increase the effectiveness of proposed model. In addition, as previously discussed, contrails and the

subsequent cirrus clouds remain the most important contributing factor towards global climate change. Based on the above reason, we believe that emphases should be placed on contrail and cirrus cloud formation control, while other sustainability measures are being refined and developed.

Currently, the flight path of commercial flights is set to optimize the fuel usage and flight time. Airlines optimized the flight path to reduce cost on fuel instead of considering the environmental impact. As less fuel is burnt, less pollutant is created. However, the weather condition is not considered, which the contrail formation is not controlled. This would possibly reduce the effectiveness of reducing pollutant emission. To mitigate the environmental problem aviation brings, the contrail formation during flight is considered in this report.

Flight time is a major factor in fuel burn and efficiency (to the airline, passengers, and aviation authority), it should be considered in the model to provide least operational cost increase to the airline and maintain airspace utilization.

Contrail is possible to form under the Schmidt–Appleman criterion; however, fulfilling the criterion does not mean that contrail would definitely form, but have a high chance of forming. Since the formation still have a linear correlation with the flying distance in area within the criterion, the contrail length can be used to estimate the amount of contrail formed.

1.2. Scope of study

There are various factors that deviate an aircraft from its intended course, namely air pressure, wind direction, wind speed, air temperature and relative humidity. The atmospheric situation (weather condition) can cause the aircraft to change its flight path, resulting in change of fuel consumption through the flight. As mentioned in the introduction, condensation trail, or contrail in short can be formed under specific atmospheric situation that flight crew should execute manoeuvre to avoid formation of such trails, such as lift or descend the aircraft. However, the lift manoeuvre can induce increase in fuel consumption as well as emission, which contradicts the intention of concerning the impact to the environment. Thus, the number of parameters would increase when more situation is considered which complicates the flight path modelling and some may contradict each other when it comes to decision making. Hence, this research focus on the parameter air pressure, air temperature and relative humidity for the construction of a simpler model. In addition, change in altitude of flight profile will only be considered instead of 3D or 4D trajectory, due to the limitation of data available.

1.3. Organization of report

The organization of this project is as follow. It starts with the research background of the topic, including the reason for the research and existing problems, objectives and scope of study. Following are literature review related to the selected topic concerning climate change, contrail and flight trajectory optimization modelling. Next are the methodologies to carry out research and the discussion of the data collected from research. Finally, conclusion will be drawn as well as future development and prospect concerning the topic will be discussed.

2. Literature Review

2.1. Aviation emission and climate change

Climate change is defined differently by the UNFCCC and IPCC [11], which UNFCCC refer it as “a change of climate that is attributed directly or indirectly to human activity that alters the composition of the global atmosphere and that is in addition to natural climate variability observed over comparable time periods”, while the latter one defines it as “a change in the state of the climate that can be identified (e.g. using statistical tests) by changes in the mean and/or the variability of its properties, and that persists for an extended period, typically decades or longer.”

The United States Global Change Research Program’s Climate Science Special Report: Fourth National Climate Assessment states that human activities induced greenhouse gases is a dominant cause of continuous global warming, resulting in many aspects of global climate changing[12].

Some of the greenhouse gases naturally exist in the atmosphere to maintain the temperature of earth by absorbing and emitting the terrestrial radiation emitted from earth surface[13]. The phenomenon is also known as greenhouse effect. Natural greenhouses gases include water vapour, carbon dioxide, nitrous oxide, methane and ozone. Besides, greenhouse gas can also be entirely anthropogenic, such as halocarbons and some fluorinated gases (F-gases). IPCC suggests that in 2010, carbon dioxide accounted for 76% of anthropogenic greenhouse gas emission, while methane, nitrous oxides and F-gases contributed to the total emission with 16%, 6.2% and 2% respectively. On the other hand, NASA research has shown that water vapour plays a significant role in the global greenhouse effect [14]. When the human activities generate the aforementioned greenhouse gases, more heat is trapped in the atmosphere. With a warmer temperature, water is vaporized more easily into the atmosphere. Given that water vapour contributes to 50% of greenhouse effect of the globe[15], it traps more heat than other types of greenhouse gases. When there is more water vapour in the atmosphere, the temperature tends to be warmer and more humid and created a spiralling cycle. As such, water vapour has an amplifying effect of greenhouse effect, global warming and to climate change. In addition, water vapour is an essential element for the formation of aircraft contrails, which the water vapour in atmosphere mixes with the hot water vapour from the exhaust of aircraft engines at low temperature and high altitude. Other than greenhouse gases, the greenhouse effect of contrail is found significant and not negligible.

By further differentiating the types of human activity that create greenhouse gases, a clearer picture of the total emission can be shown. According to the research done by IPCC in 2010, the sources of greenhouse gas emissions can be classified into different economic sectors[16]. For direct greenhouse gas emission, electricity and heat production contributes to 25% of emission, followed by agriculture, forestry and other land use (AFOLU) with 24%, industrial process with 21%, transportation with 14%, other energy with 9.6% and buildings with 6.4%. With the data provided by ICAO, it is estimated that aviation industry contributes to 3%

of climate change induced by anthropogenic radiative forcing [17].

With the continuous increase in concentration of greenhouse gas, the natural greenhouse effect of the globe is driven to an imbalance state, resulting in an increase in the average global temperature. For instance, the averaged combined land and ocean surface temperature has been risen by 0.85 °C in the period of 1880 to 2012 [16]. IPCC also stated the increased temperature has led to increased frequency of extreme weather events, such as drought and storm surge. As a result, the overall climate has been changed due to the greenhouse gases emitted from human activities.

One type of aircraft emission is nitrogen oxides, which are formed from nitrogen reacting with oxygen in the high temperature condition of aircraft engines. On the other hand, given that aircraft engines use derivatives of petroleum, such as diesel, kerosene and aviation gasoline (avgas), which are fuels mostly composed of hydrocarbons. Incomplete combustion of these fuels in the aircraft engine combustion chamber will result in the emission of some of the unburnt carbons, also known as soot. In addition, when there is sulphur contained in the aircraft fuels, the combustion of these fuels will emit sulphur dioxide and some small proportion of oxidized H_2SO_4 . The condensation of soot and sulphur-contented will result in sulphate aerosol, which influences the formation of clouds [18]. Last but not least, combustion of hydrocarbons has the major products carbon dioxide and water vapour. The former has a well-understood significance on climate change as a greenhouse gas, while the latter's influence is still under research in recent decades. Another issue correlated to water vapour is the formation of contrail cirrus. When the hot water vapour is emitted from aircraft engine at high altitude with low temperature, it condenses rapidly and mixes with the ambient air with lower water content and forms aircraft contrails and cirrus clouds.

As mentioned, aircraft engines emit various types of gases and each has their respective impact to climate change.

As for nitrogen oxides, itself is a greenhouse gas which demonstrates characteristics of trapping long-wave radiation in atmosphere. Other than that, it perturbs the formations and compositions of other two greenhouse gases in the atmosphere, namely methane and ozone. Methane, which is a type of volatile organic compound, reacts with nitrogen oxides under sunlight to form ozone and some other products[19]. The reaction involves multiple steps:

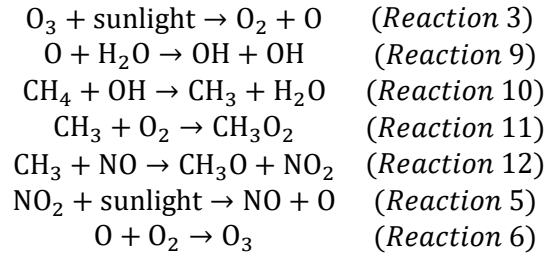


Figure 6. Ozone Formation [18]

As such, it can be demonstrated that the composition of methane and nitrogen oxide can perturbate the formation of ozone. As aircraft engine can emit nitrogen oxide which affects the composition of ozone and methane, it has a certain contribution to climate change. According to Frömming et. al. [20], ozone and methane have radiative forcing values of 67.4 mWm^{-2} and -34.4 mWm^{-2} to climate change in one of their predicted scenarios respectively. As for water vapour and carbon dioxide in the same scenario, the radiative forcing values are 6.9 mWm^{-2} and 101.3 mWm^{-2} respectively.

According to Detwiler and Jackson [21], “contrails form in the exhaust plumes behind aircraft powered by engines burning hydrocarbon fuels when they fly in sufficiently cold and humid air.” It also has another variant, which is formed at the sharp surfaces, such as wing tips when the aircraft is entering very humid air. The former is named exhaust contrail and the latter is named aerodynamic contrail.

Exhaust contrail is a type of cloud which is formed by mixing unsaturated warmer air in high ratio of water vapour with unsaturated cooler air with low ratio of water vapour. Water saturation is then attained temporarily and forms liquid droplets that quickly freezes due to the low temperatures in the upper troposphere [22]. The condition for water to be saturated to form contrail is known as Schmidt-Appleman criterion, with parameters of relative humidity, temperature, ratio of exhaust gas to environment, air pressure and amount of water emitted from combustion of fuel. Appleman [23] studied the phenomenon and stated that “not only necessary for the water vapor from the fuel combustion to raise the relative humidity of the entrained environment to 100 percent with respect to water, but also some visible water must be produced.”

Through applying the process onto the condition of aircraft engines, water vapour, carbon dioxide and other unburnt particles are first emitted to the atmosphere after the combustion of hydrocarbon fuels in combustion chambers. The water vapour then almost freezes instantaneously on the surfaces of ambient ice crystals, which is the state of water at high altitudes. If such freezing nuclei is not available for the transition of water to ice, the soot in the exhaust gas will instead supply the nuclei for such transition. As such, the contrail that once had 100% relative humidity with respect to water would be supersaturated with respect to ice. The excessive water vapour then continuously freezes to ice, until an approximately 100% of relative humidity with respect to ice is attained. The contrail may then persist, spread in sheared wind field and extend its area to form contrail cirrus

[22].

For aerodynamic contrails, it can be triggered from accelerated air flow with decreasing local temperature. Due to the conservation of energy, the objects that once accelerates will experience a cooling effect, where water vapour in the environment that once accelerated will be cooled altogether. When applying the phenomenon to a moving aircraft, it can be realized that high-g manoeuvres, such as lifting can generate short-lived clouds at the sharp edges of aircrafts like wingtips and flaps. This is a result from the decrease in pressure and temperature after the passage of the mentioned aircraft structure and leads to condensation of water vapour in the air [22]. The phenomenon is called short-lived as the contrail often disappears shortly at near ground due to the temperature does not favour the condensed water vapour, or ice to sustain. However, when it comes to high altitudes where ambient temperature is sufficiently cold, it is likely the contrail will sustain longer after the passage of aircraft on the condition of ambient air saturated with ice.

As mentioned, some young or newly formed contrail can spread out due to wind shear and form contrail cirrus. Although they share same origin, their contribution to climate change is not the same at all. With reference to Burkhardt and Karcher [2], the global long-wave radiative forcing contributed by young contrails is around 5.5 mWm⁻² while the short-wave radiative forcing is -1.2 mWm⁻², resulting a net radiative forcing of 4.3 mWm⁻². On the other hand, contrail cirrus generates long-wave radiative forcing of 47.1 mWm⁻² and short radiative forcing of -9.6 mWm⁻², resulting a net radiative forcing of 37.5 mWm⁻². When compared with young contrail, contrail cirrus has about 9 times larger of radiative forcing.

2.2. Optimization model

Trajectory optimization is used in aviation to minimize the flight time, fuel usage and maximize the payload through adjusting the control variable, such as AOA and thrust, against the state variable, such as position and mass [24, 25]. A basic model of the optimal control problem would be solving a nonlinear differential equation describing the dynamic system, i.e.,

$$\dot{x}(t) = f(x(t), u(t), t), t_0 \leq t \leq t_f$$

A 2D flight trajectory model would normally consider the change in flight level. It is used to minimize the operational cost, mostly on fuel, during a particular flight segment. This is possible as fuel consumption reduce with altitude increase under troposphere for all aircraft engine due to the relation of TAS with altitude [26]. The existing algorithms used in FMS would divide the cursing distance into different segments and consider the best flight level with minimising both segment flight time and fuel burn rate [27]. The wind compounds in these models are considered as affecting the horizontal distance only. A simple form of a 2D trajectory model would be dependent on the TAS, ascent/descent rate and wind condition putting into the aircraft performance model to

1 estimate the flight time and fuel efficiency.

2
3 A 4D trajectory model would consider the horizontal and lateral motion of the aircraft to optimise the flight time
4 and fuel burn through planning for the flight path and envelop. In the model, the aircraft is described through
5 equation of motion, stating the variables to derive the translational motion of the aircraft. Different sub-model
6 describing factor such as fuel burn, geographical data and weather is used to set the limitation and goals.
7 Through solving the differential equations, the optimized route is derived for the flight segment [28]. In more
8 recent research, many have use 4D trajectory model for multi-objective optimization, for better efficiency not
9 only in the fuel consumption, but also to avoid certain terrain or weather. For more advance usage of these
10 model, the airspace and airdrome utilisation are considered, such as in 4D air traffic management where the
11 arrival time is controlled through mathematical formulation [29]. A 4D flight trajectory would bring a higher
12 flexibility and degree of control than only controlling the flight level, for a more accurate relation of the weather
13 and aircraft is defined, and more flight path options in a 3D space.

14
15 On 2D trajectory optimization, Dancila et. al. [30] have proposed an analytical approach using energy-state
16 equation to search for the best flight altitude for cruising considering the flight cost and fuel consumption. This
17 method is validated through comparing with CMC – Electronics Esterline CMA9000-PTT. Dancila and Botez
18 [27] have used graphical model to simulate the possible flight route of an aircraft to optimize the flight level
19 under predicted wind condition against fuel burn. For 3D/4D trajectory optimization, Mendoza [31] have used
20 numerical approach, through developing a “five routes algorithm” to compare the performance to the objectives
21 of different possible route. This approach is compared with the PTT data of L-1011 and RRJ 100, showing an
22 improvement of 1.89% And 0.62% respectively. The algorithm used is also faster than using bilinear
23 interpolation by 30%, making it possible to be implemented onboard in the FMS. Dougui et. al. [32] proposed
24 a light propagation model for optimization of trajectory to avoid conflict. The result is compared to genetic
25 algorithm on the classic 6 aircraft converging towards the centre of a circle trajectory optimization problem,
26 which shown a similar result with less computational time, proving the potential of this algorithm being a quick
27 solution to trajectory conflict optimization. Wickramasinghe et. al. [28] attempted to use dynamic programming
28 to calculate the optimized path with performance index which consider the fuel flow and weather. The optimal
29 route is compared with the actual flight data on the flight route between Fukuoka and Haneda, showing a slight
30 increase in flight time (less than 300 second on average) while having to use on average about 10% less fuel,
31 reducing aircraft emission. Gardi et. al. [29] used the optimization control problem direct method to solve the
32 trajectory problem. This research is multi-objective, on the operational, economic and environmental factor,
33 involving the calculation of partial differential equations, Pseudo-spectral methods are used to resolve the
34 mathematical model. González-Arribas et. al. [33] used robust optimal control to predict the optimal trajectory
35 under uncertain wind condition. They adopted the stochastic quadrature rule to assemble the continuous
36 probabilistic function to discretized probabilistic function for better estimation. Murrieta-Mendoza et. al. [34]
37 optimized the fuel burn and flight time through graphical method. A unidirectional graph is established to reflect

all possible route to the flight. The result is compared with real flight data, showing a reduction in fuel burn from 1.99% to 7.22%, and a reduction in flight time from 0.25% to 2.72%. Serafino [35] have also used a graphical method for trajectory optimization in avoiding adverse weather and reduce aircraft emissions. The result is compared using Pareto front under Dijkstra and genetic algorithm respectively. Rosenow and Fricke [36] have also used the graphical method to solve the optimization problem of flight trajectory, but with a different architecture and algorithm. Using the platform Toolchain for Multicriteria Aircraft Trajectory Optimization (TOMATO), which is a graphical based model using the A* algorithm, the trajectory is optimized against contrail. The model is compared with models done in other studies, showing same order of magnitude in the result, validating the model. Other researchers have tried to use biological evolution to improve the 4D optimization calculation. Yin et. al. [37] have used genetic algorithm to reduce the persistent contrail formation in flight. The model is built based on the ECHAM/MESSy Atmospheric Chemistry (EMAC) with the sub-model AirTraf and optimized with the Adaptive Range Multi-objective Genetic Algorithm, showing that contrail distance can be reduced significantly with little increase in flight time and fuel consumption. Patrón et. al. [38] have used genetic algorithm to couple the vertical and lateral profiles optimization to reduce fuel burn in term of cost. The use of GA has allowed a reduction in calculation time, making the possibility for the model to be implemented to the FMS. The result is compared with 20 real flight data, showing a reduction in cost of 5.6% on average.

2.3. Aircraft performance model

An aircraft performance model describes the characteristic of the aircraft using the performance data of the aircraft. It would reflect the aerodynamic and propulsion characteristic under different situation, such as altitude, air speed and AOA. This model can be constructed based on different methods, such as equation of motion, total energy model or other mathematical models.

The model is based on the aerodynamic motion of the aircraft. Depending on the usage, the model can be a simple 1DOF motion model, up to 6DOF motion model for full aircraft dynamic control. These equations are converted to a state-space model for control theory calculation [39]. For trajectory optimization problem, a 3DOF model is most commonly used. A general form of a 3DOF flight dynamics differential algebraic equations is described by Gardi et.al. [29] :

$$\begin{cases} \dot{v} = g(T/W - D/W - \sin\gamma) \\ \dot{\gamma} = \frac{g}{v} \cdot [N \cos\mu - \cos\gamma] \\ \dot{\chi} = \frac{g}{v} \cdot \frac{N \cos\mu}{\cos\gamma} \\ \dot{\phi} = \frac{v \cos\gamma \cos\chi + v_{w\phi}}{(R_E + Z) \cos\phi} \\ \dot{z} = v \sin\gamma + v_{wz} \\ \dot{m} = -F \end{cases}$$

Total energy model is built based on the relation of geometrical (potential) and kinematic energy with the aircraft motion. It calculates the rate of work done (energy transfer) with the energy equation: $(T - D)v = W\dot{h} + mv\dot{v}$ [40]. As the mass of the aircraft is change with fuel consumption, the two equations can form into an ODE system. This model is completed with formula describing the flight profiles with speed $\dot{r} = v \cos\gamma$, aircraft performance and operation model.

Fuel burn model is implemented to calculate the fuel flow, which can be used to model the dynamic gross weight reduction of the aircraft and the amount of aircraft emission.

Mendoza et.al. [34] have developed a fuel burn model in cruising phase with constant altitude and change in flight levels using simple aerodynamic equations with aircraft performance data from BADA: *Fuel flow* =

$$\frac{\frac{\rho}{\rho_0} \cdot \left(\frac{t}{t_0}\right)^{\frac{1}{2}} \cdot M_{ref} \cdot g_0 \cdot a_0}{L_{hv} \cdot C_f} \cdot \text{Comprehending this equation with thrust at climb and descent and rate of climb/descent gives}$$

the fuel flow at throughout the cruising stage.

Dancila et. al. [30] developed the fuel burn model with three modules, initialization module, intermediary module and the fuel burn module. The initialization module is used to setup several auxiliary tables based on the aircraft gross weight and fuel volume before take-off. The intermediary module setup an ISA and Mach-based fuel burn look-up table with the information from the initialization module and flight information, renewing once every speed or standard temperature deviation changes. The final module calculates the fuel burn based on the information from the previous modules with the evaluated cruise altitude and estimated flight time on that segment of flight.

A weather model is to represent the weather and climate of the segment area through historical data. Depending on the goal, the complexity would be different. For example, if the optimization is on altitude and fuel, wind can be the only factor in the weather model [40]. However, if the optimization is multiobjective and needed to be more accurate, other factors, such as temperature, air density and humidity, may be necessary [35]. As the weather information is not a continuous data, which is the data is measured in selected point for a fixed period of time, mathematical methods, such as normalizing and interpolation, may be needed for generating a continuous weather model with higher resolution [38].

Flight cost model is used to calculate the flight cost. To isolate this model from the fuel price at the time, it is calculated in term of weight of fuel. Cost index (CI) is used to complete the cost model, translating the flight time (time cost) in term of fuel cost providing the priority of time cost when summing up with fuel cost to calculate the total flight cost. This index would affect the preferred airspeed in the optimization problem. If time is less important, CI would low, resulting in lower airspeed to reduce fuel consumption, vice versa [34]. The basic form of flight cost would be,

$$\text{Flight cost} = \text{total fuel cost} + CI \times \text{flight time}.$$

As the data obtain, such as weather and aircraft performance, are discrete information, to import to the optimization model, these data needed to be normalized or interpolated to obtain a continuous information.

3. Methodology

The proposed model considers the optimization problem in a 2D space based on a direct graphical model, which would consider all possible route within the limitation defined based on application. The model balances the contrail length and fuel consumption through altering the flight level to avoid certain areas. The model is separated into several sub-models, namely contrail sub-model, fuel consumption sub-model, and aviation traffic flow model, based on the goals and main factor.

3.1. Graphical model

In the case of a commercial flight, the route of a flight consists of 3 stages, climb, cruise and descent. The model proposed in this report control the cruising of the aircraft. We assume in this stage of flight is: 1. the aircraft

would only fly forward to the destination without moving backwards or alternating from the original route, 2. the aircraft would be flying in certain altitude/ flight level and would not fly in between levels (the flight level used would be depending on the local authority normal practices), 3. the aircraft would pass through the same waypoints defined in the FIR in every same flight in the horizontal space. To mimic this characteristic of this stage of flight a direct graphical model is chosen.

3.1.1. Direct Graphical Model

The proposed 2D direct graph is defined by the ground distance and the altitude. In the graph are filled with finite number of nodes/waypoints which are evenly distributed along the space. The number of nodes/waypoints would affect the resolution of the model. This model is represented with the search space as graph $G(E,V)$, where E denotes the linkage between two waypoints of consecutive column and V representing the waypoints. This model would allow many different combinations of path through passing different E ; however, as the model is directional, it only allows the aircraft to pass through one E in each segment of ground distance.

3.1.2. Source and Sink

In a direct graph, a single source and sink is needed respectively; however, an aircraft is free to define its top of climb (ToC) and top of descent (ToD). Therefore, the source and sink are defined in this model as zero distance to any waypoints in the first column and to any waypoints in the last column respectively. This would allow the model to propose the ToC and ToD, instead of using fix ToC and ToD, providing flexibility and more options of path, further optimizing the trajectory.

3.1.3. Model Boundary

Theoretically, this model would have infinite waypoints for infinite space above ground. To meet the reality where commercial aircraft would not fly pass the troposphere, the vertical boundary is limited between 41000ft and 35000ft from MSL to meet the normal cruising height of civil aviation. As only the cruising stage is concerned in this report, the horizontal boundary is limited from the start to end of the cruising of the flight.

3.2. Contrail estimation

The weather data is obtained from China Weather Stations, where the essential parameters for modelling are available, such as relative humidity, air pressure and air temperature. As the weather data are representing the condition of a discrete point, there are gaps to be filled between those points. To obtain a more complete picture for modelling, interpolation of these data is required, which would be further discuss in section 3.5.2.

As mentioned in part 3.1.1 and 3.1.3, the selected air route would be divided horizontally to a number of sectors J and vertically in different flight levels I . The fixed air route can then be managed using flight levels $i_1, i_2, \dots, i_J \in I$ and with air route sectors $j_1, j_2, \dots, j_J \in J$. The meteorological data and weather information will

be provided by the major cities along the selected air route, with parameters of air pressure, relative humidity with respect to water vapour and ice, air temperature at different flight levels and air route sectors. As such, the contrail sub-model should have a higher resolution than the ATFM sub-model, in order to obtain an optimized flight path with higher accuracy. In addition to weather factors, the parameters also include contrail formation threshold value, the estimated threshold temperature for contrail formation at different flight levels and air route sectors. A function of saturation vapour pressure over water at given temperature will also be included.

Table 1

Contrail formation sets and parameters

Set	Description
I	A set of flight levels (indexed by i_1)
J	A set of air route sectors (indexed by j_1)
Parameters	Description
$P_{i_1 j_1}$	Air pressure (Pa) at flight level i_1 and air route sector j_1
$RH_{i_1 j_1}^w$	The relative humidity to water at flight level i_1 and air route sector j_1
$RH_{i_1 j_1}^i$	The relative humidity to ice at flight level i_1 and air route sector j_1
$T_{i_1 j_1}$	The temperature at flight level i_1 and air route sector j_1
$r_{i_1 j_1}^{contr}$	The contrail formation threshold value at flight level i_1 and air route sector j_1
$t_{i_1 j_1}^{contr}$	The estimated threshold temperature for contrail formation at liquid saturation at flight level i_1 and air route sector j_1
$e^{liq}(T)$	A function of the saturation vapor pressure over water at given temperature T

The calculation of contrail formation involves the above parameters and the following equations.

$$r_{i_1 j_1}^{contr} \leq RH_{i_1 j_1}^w \leq 100\%, \forall i \in I, \forall j \in J \ \& \ RH_{i_1 j_1}^i \geq 100\%, \forall i_1 \in I, \forall j_1 \in J \quad (1)$$

The above is the equation for the formation of contrail, where the ambient relative humidity of water and contrail formation threshold value 100% at max while the ambient relative humidity of ice is at least 100%. The ambient relative humidity of water will be directly obtained from meteorological data, while the contrail formation threshold value is computed as follows:

$$r_{i_1 j_1}^{contr} = \frac{G_{i_1 j_1}(T_{i_1 j_1} - t_{i_1 j_1}^{contr}) + e^{liq}(t_{i_1 j_1}^{contr})}{e^{liq}(T_{i_1 j_1})}, \forall i_1 \in I, \forall j_1 \in J \quad (2)$$

Where $T_{i_1 j_1}$ is the temperature at the flight level i_1 and air route sector j_1 , $t_{i_1 j_1}^{contr}$ is the estimated threshold temperature for contrail formation at liquid saturation and $e^{liq}(T)$ as a function of

saturation vapour pressure over water at given temperature T. The variables are calculated as follows:

$$t_{i_1 j_1}^{contr} = -46.46 + 9.43 \log(G_{i_1 j_1} - 0.053) + 0.72 \log^2(G_{i_1 j_1} - 0.053) \forall i_1 \in I, \forall j_1 \in J \quad (3)$$

$$G_{i_1 j_1} = \frac{El_{H_2O} G_p P_{i_1 j_1}}{\varepsilon Q (1 - \eta)}, \forall i_1 \in I, \forall j_1 \in J$$

, where $El_{H_2O} = 1.25$

$$G_p = 1004 [j \text{ per } kg] \quad (4)$$

$$\varepsilon = 0.6222$$

$$Q = 4.3 \times 10^6 [j \text{ per } kg]$$

$$\eta = 0.15$$

$$e^{liq}(T) = e_0 \times 10^{\frac{7.5T}{237.3+T}}, \text{ where } e_0 = 6.11 \text{ hPa} \quad (5)$$

As for relative humidity of ice, it is not provided from meteorological data but the following calculation instead:

$$RH_{i_1 j_1}^\eta = RH_{i_1 j_1}^w \frac{6.0612 \exp \frac{18.102T_{i_1 j_1}}{249.52 + T_{i_1 j_1}}}{6.1162 \exp \frac{22.577T_{i_1 j_1}}{237.78 + T_{i_1 j_1}}} \quad (6)$$

1

2 hPa is the symbol for hectopascal and SI unit of pressure and stress equal to 10^2 pascals.

$$3 \quad 1 \text{ hPa} = 100 \text{ Pa}$$

$$4 \quad 1 \text{ Pa} = 1 \text{ N/m}^2 = 1 \text{ kg.m.s}^{-2}/\text{m}^2$$

5

6 The contrail formation at flight level i_1 and air route sector j_1 is subject to two condition, as shown in Equation
7 (1). The first condition is that the relative humidity to water $RH_{i_1 j_1}^w$ is larger than the threshold of contrail
8 formation $r_{i_1 j_1}^{contr}$. The second condition is that the relative humidity to ice $RH_{i_1 j_1}^i$ is larger than or equal to
9 100%. The threshold of contrail formation is calculated by Equation (2), which is associated with the function
10 of saturation vapor pressure over water at temperature $T_{i_1 j_1}$ and the function of saturation vapor pressure with
11 respect to the temperature threshold $e^{liq}(t_{i_1 j_1}^{contr})$. The temperature threshold $t_{i_1 j_1}^{contr}$ is calculated by Equation
12 (3), the $G_{i_1 j_1}$ is estimated by Equation (4) and the function of saturation vapor pressure is calculated by
13 Equation (5). The relative humidity to ice is subject to the relative humidity to water $RH_{i_1 j_1}^w$ and the temperature
14 $T_{i_1 j_1}$, as shown in Equation (6).

3.3. Aviation Traffic Flow Management Sub-model

The ATFM sub-model being defined in the 2D space, M denoting the set of flight levels where m_1 is the first level followed by m_2/m_{1+1} , and N denoting the set of air route sectors where n_1 is the first sector followed by n_2/n_{1+1} . The objective of this model is to minimize the presence of contrail, the optimized path is chosen with the least amount of contrail length sum up from each segment, which is found by the contrail sub-model. Equation (7) sums up the contrail length from all the chosen path, i.e., $l_{r_{m_1 n_1} r_{m_2 n_2}}^{contr}$ for the E between $r_{m_1 n_1}$ and $r_{m_2 n_2}$, through comparing with other possible combinations, resulting in an optimized route, $\min z_0$.

$$\min z_0 = \sum_{n_1}^{N-1} \sum_{m_1}^M \sum_{m_2}^M l_{r_{m_1 n_1} r_{m_2 n_2}}^{contr} y_{r_{m_1 n_1} r_{m_2 n_2}} \quad (7)$$

s. t.

$$r_{m_s n_s} = 1 \quad (8)$$

$$r_{m_d n_d} = 1 \quad (9)$$

$$\sum_{m_1}^M r_{m_1 n_1} = 1, \forall n_1 \in N \quad (10)$$

$$\sum_{m_1-k}^{m_1+k} r_{m_1 n_1+1} \leq r_{m_1 n_1}, \forall m_1 = k, \dots, M-k, \forall n = 1, \dots, N-1 \quad (11)$$

$$r_{m_1 n_1} + r_{m_2 n_2} \geq y_{r_{m_1 n_1} r_{m_2 n_2}} - 1, \forall n_1 = 1, \dots, N-1, \forall n_2 = 2, \dots, N, \forall (r_{m_1 n_1}, r_{m_2 n_2}) \in E \quad (12)$$

$$h_{n_1 n_1+1} \geq r_{m_1 n_1} + \sum_{m_2, m_2 \neq m_1}^M r_{m_1 n_1+1} - 1, \forall n = 1, \dots, N-1 \quad (13)$$

$$\sum_{n_1}^{N-1} h_{n_1 n_1+1} \leq H \quad (14)$$

Constraints (8) and (9) defines the source and sink of the graph respectively, the points are considered as zero distance from the first and last waypoint, the value are regarded as 1 as the aircraft must pass through these two points in the model to enter the cruising stage. Constraints (10) defines that only one waypoint can be used in each air route sector, which is to describe that an aircraft would only be in one flight level in each section of flight. In Constraints (11), the k value is the remaining maximum number of times the aircraft can change its altitude in the model. This formula ensures that the maximum times of flight level change during cruising would not exceed the maximum value. Constraints (12) introduce the decision variable $y_{r_{m_1 n_1} r_{m_2 n_2}}$ to connect the relation of two waypoints, defining the edge between the two waypoints are selected or not. Constraints (13) and (14) using the auxiliary variable $h_{n_1 n_1+1}$ to indicate whether flight level changed between the sector n_1 and n_{1+1} , making sure that the maximum number of flight level changes would not exceed the user-defined maximum number H . Having a large H would possibly increase the workload of pilot and the ATM system and should be

set according to normal practices and realistic system capability.

Table 2

Notations and decision variables.

Set with indices	Description
G	A directed graph consisting of a nonempty vertex set of waypoints V and an edge set of air route E
V	A vertex set of waypoints (indexed by $r_{m_s n_s}, r_{m_1 n_1}, r_{m_d n_d}$)
E	An edge set of air route (indexed by a pair of $(r_{m_1 n_1}, r_{m_2 n_2})$)
M	A set of flight levels (indexed by m)
N	A set of air route sectors (indexed by n)
π	A set of paths from artificial source waypoint $r_{m_s n_s}$ to artificial sink waypoint $r_{m_d n_d}$
Parameters	Description
$r_{m_s n_s}$	Artificial source waypoint ($r_{m_s n_s} \neq r_{m_d n_d}$)
$r_{m_d n_d}$	Artificial sink waypoint ($r_{m_s n_s} \neq r_{m_d n_d}$)
$l_{r_{m_1 n_1} r_{m_2 n_2}}^{contr}$	A non-negative contrail length on air route $(r_{m_1 n_1}, r_{m_2 n_2})$
k	The maximum tolerance of flight levels changes after passing through an air route sector n_1
H	The maximum number of flight levels changes in a path $\langle r_{m_s n_s}, \dots, r_{m_d n_d} \rangle$
Decision or auxiliary variables	Description
$P_{r_{m_s n_s} r_{m_d n_d}}$	A path $\langle r_{m_s n_s}, \dots, r_{m_d n_d} \rangle$ from source waypoint $r_{m_s n_s}$ to destination waypoint $r_{m_d n_d}$ in a digraph G
$r_{m_1 n_1}$	1, if flight is assigned to path through the waypoint at flight level m_1 and air route sector n_1 ; 0, otherwise.
$h_{n_1 n_1+1}$	1, if the flight levels have changes from air route sector n_1 to $n_1 + 1$; 0, otherwise.
$y_{r_{m_1 n_1} r_{m_2 n_2}}$	1, if flight pass through from waypoint at flight level m_1 and air route sector n_1 to waypoint at flight level m_2 and air route sector n_2 ; 0, otherwise.

3.4. Open Aircraft Performance Model (OpenAP)

To acquire aircraft data for the simulation processing, OpenAP was chosen as the aircraft performance model.

OpenAP is an open model that combines open data, literature models as well as estimated parameters originating

from open data[41], where use of open aircraft surveillance data is a unique characteristic of the model. There are four major components for the model, namely aircraft and engine properties, kinematic performances, dynamic performances and utility libraries.

For aircraft and engine properties, the model has included common aircraft types characteristics, such as nominal cruise conditions, dimensions, weights, limits and engine options, where these data are based on public data given by aircraft manufacturers. And there are around 400 engines included in the databases of OpenAP, which each engine comprises of 11 parameters concerning its performance, including name, manufacturer, bypass ratio, maximum thrust, fuel flow etc. The source of data for the engines is ICAO aircraft engine emissions databank.

For Kinematic performances, the model studies the motion of the aircraft by dividing the entire flight into 7 phases, where different performance parameters at each phase is modelled accordingly. To indicate the performance of the aircraft in the model, there are indicators of altitude, distance, acceleration, vertical rate and speed. As such, A trajectory of a flight through take off until landing can be described.

To stretch the OpenAP capabilities further, the dynamic model was introduced. Other than dividing the flight into different phases, the dynamic model includes more performance parameters, specifically mass and forces, which includes computation of gravity, thrusts, drags, flaps, compressibility and fuel flow. Not only is the computation done by their corresponding laws of physics, but also are models from literature and open flight data used in OpenAP, such as the mentioned engine emissions databank provided by ICAO.

For the utility libraries, OpenAP provides flight phase library, it provides the entire flight trajectory from take off to landing for users to obtain. For aeronautical calculations, it derives data from the open source BlueSky simulator, which functions for computing bearing and distance. For Navigation database, it acquires data published by X-Plane, which gives information on airport and navigation data.

When compared to the most common aircraft performance model Base Of Aircraft Data (BADA), OpenAP has the edge of slightly higher accuracy, especially in a high thrust situation, such as climbing phase. More importantly, it is an open source which does not required the authorisation like BADA. Thus, OpenAP is chosen as the aircraft performance model for the required simulation.

3.5. Weather Map plotting

As weather data are not continuous data and only show the condition of a small area around the weather station, the resolution of the data is low and uneven. It is necessary to use mathematical method to estimate the weather condition of each points in the map evenly.

3.5.1. Weather Station

There are several parameters concerned when it comes to studying the condition that favours the formation of contrail, namely humidity, temperature, ratio of exhaust gas to environment, air pressure and amount of water emitted from combustion of fuel. Thus, humidity, temperature and air pressure of the atmosphere which the designated flight will pass through have to be obtained for the sake of optimization of the flight path, in regard to mitigate the formation of contrail. To obtain the weather data, the weather station along the chosen flight path has been selected to be the data source. The location of the weather stations is shown in **Figure 7**.

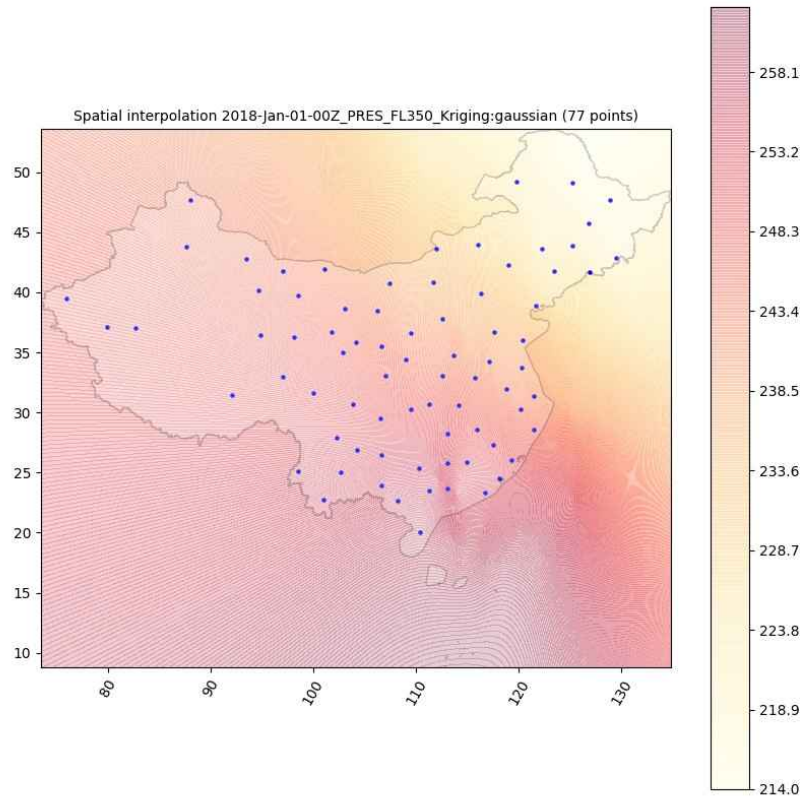


Figure 7. Weather station location (blue dots) and spatial air pressure

3.5.2. Kriging method

Kriging is a kind of interpolation method that consider the geographical location of data as the factor to estimate the data of other location[42]. The general formula is as below:

$$Z := \sum_{\alpha=1}^N \lambda_{\alpha} Z_{\alpha} \quad (15)$$

Where: λ is the weighting of the geographical location and Z is the measured value.

In the case of weather data, Kriging is a more suitable option than other interpolation, such as bilinear interpolation, which is commonly used for increasing the resolution of the data. This is because weather stations are irregularly distributed and so is the data obtained. To increase the reliability of the estimation, data from all weather station available are considered, using Kriging can have a better relate the estimated result with the geographical location of the points.

To simulate the correlation of the weather condition of different points, linear kriging is chosen, as the temperature, humidity and temperature is the differ mostly linearly from one point to another. The kriging method used only consider the data on the same flight level to reduce the processing time.

3.6. Path Optimization with Contrail Mitigation

As mentioned in section 3.2 and 3.3, it is a two process calculation: first to get the weather map of each flight levels (contrail sub-model), second to find the optimized flight path with minimum contrail length through manipulating the maps obtained from the first part (ATFM sub-model).

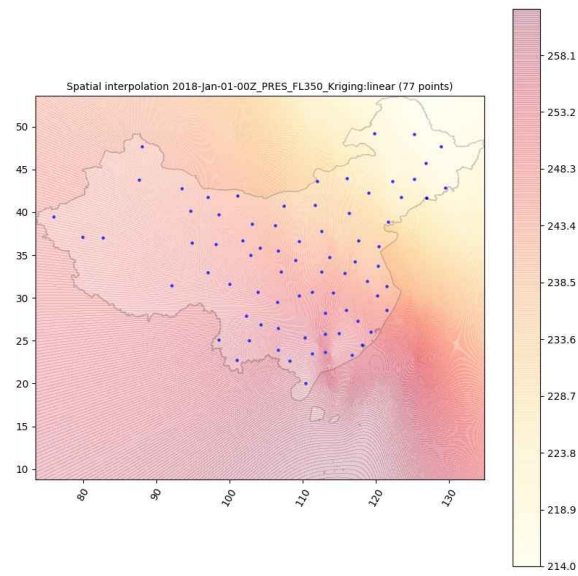
3.6.1. Up Scaling of Meteorological Data

The purpose of this function is to generate a map in each flight level of the selected time showing the area that have a high chance of producing contrail when an aircraft passes through with the data from 3.6.1. The result is a grid of Boolean value. This process would be runed once for every point on the graph with each set of data. These Boolean values would be organized by flight level and used to generate the corresponding graphs and csv files for later trajectory optimization and contrail size estimation. These data would show the areas having a high change of contrail creation at the given time on each flight level, as shown in Error! Reference source not found..



Figure 8. Defining Contrail Area into a Map

1

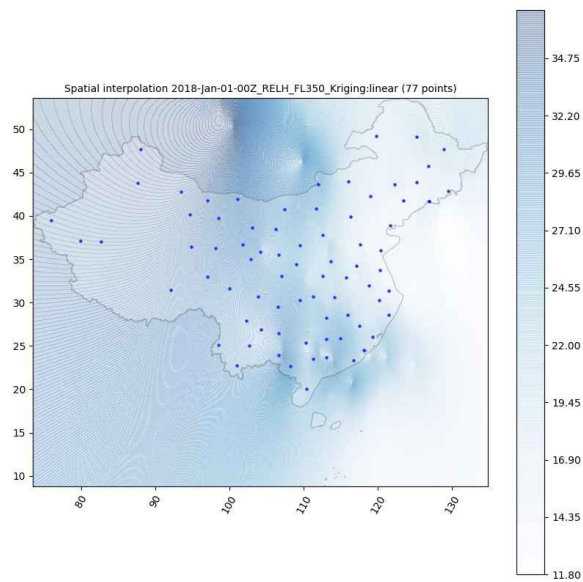


2

3

Figure 9. Spatial interpolation of air pressure on 1st Jan 2018 at flight level 350

4



5

6

Figure 10. Spatial interpolation of relative humidity on 1st Jan 2018 at flight level 350

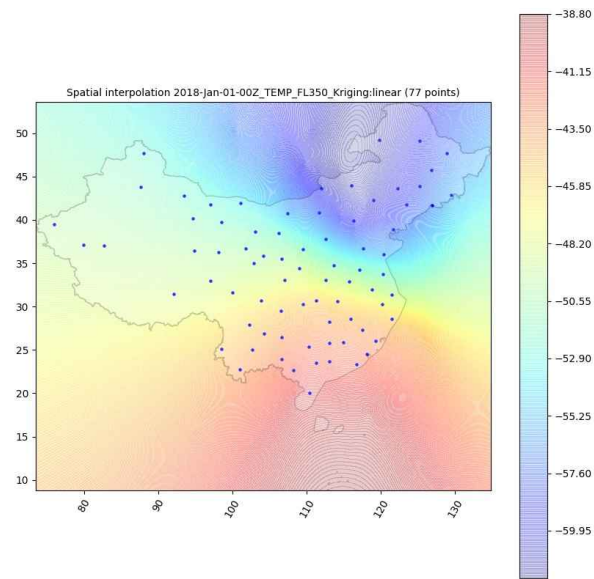


Figure 11. Spatial interpolation of template on 1st Jan 2018 at flight level 350

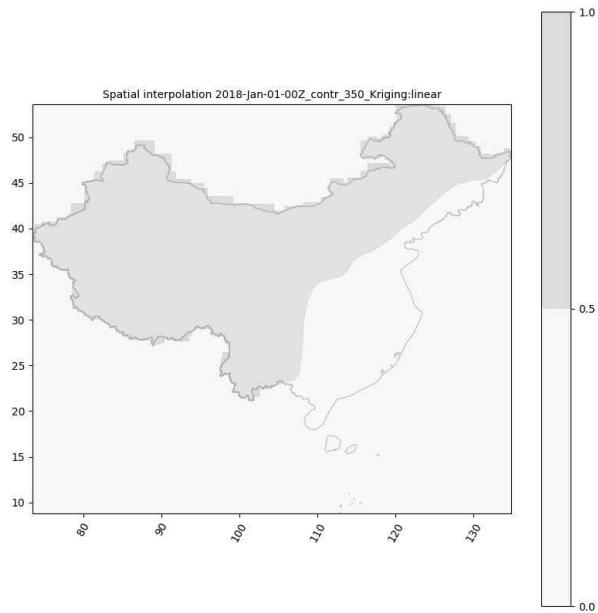


Figure 12. Spatial interpolation of contrail formation criteria on 1st Jan 2018 at flight level 350

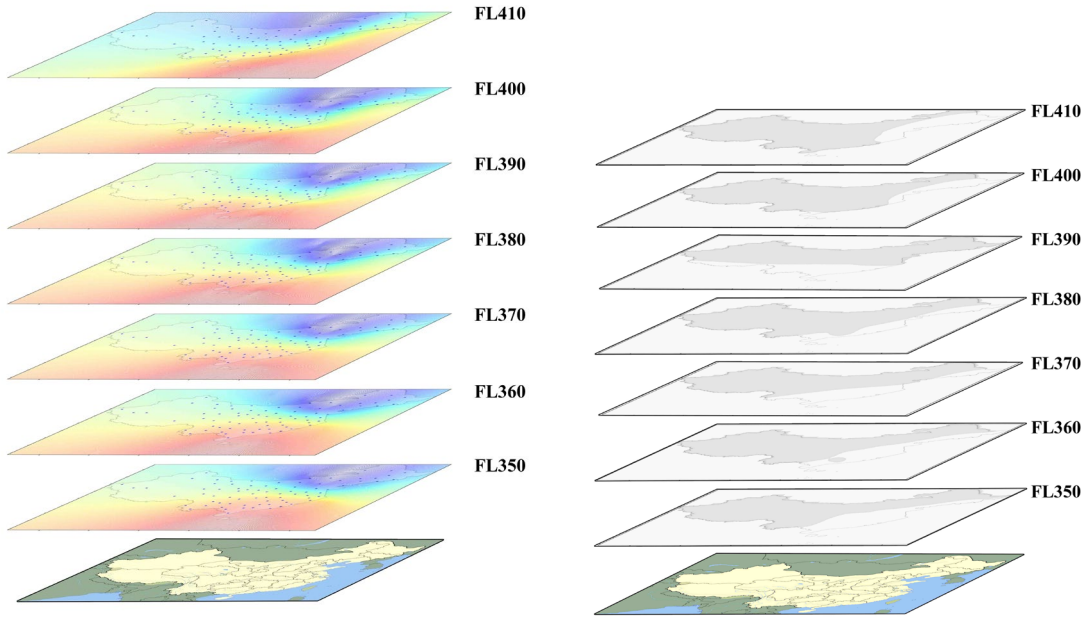
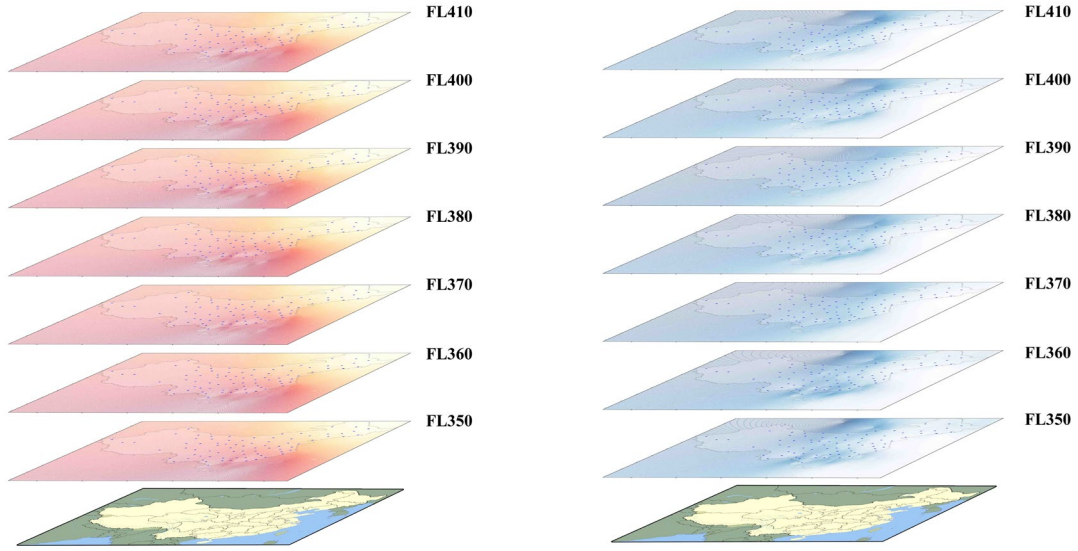


Figure 13. 3D view of spatial interpolation

3.6.2. OpenAP Flight Trajectory

The trajectory generation function is based on the architecture of OpenAP [41] and WRAP [43]. OpenAP provided the data of aircraft and performance of specific aircrafts commonly used in civil aviation. By using the library of OpenAP, the aircraft flight performance of a selected path is calculated to provide the necessary parameter for the predicting the trajectory, which is part of the kinematic performance model which calculates climbing performance. The parameters of the whole path are combined to generate the trajectory.

3.6.3. Flight Path Optimization

The final flight path is generated by referring to the trajectory calculated through the OpenAP with the waypoint data containing the actual geographic location of useful waypoint of selected flight. This program assumed that the aircraft would only carry out flight level change (ascent or descent) when passing through a waypoint if deemed necessary.

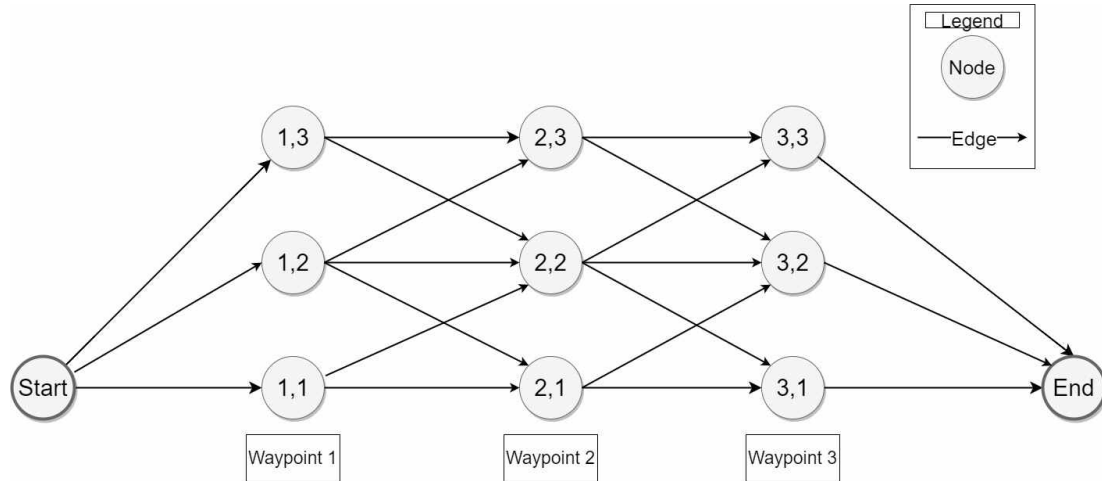


Figure 14. Direct Graph Model

As stated in section 3.1.1, this paper is developed under direct graph model. Through NetworkX library, the waypoints are described into a direct graph with different flight level as a separate point. **Figure 14** shows the process of building up the direct graph network, describing the edges from one node to another. With the “all_simple_paths” function from the library, we can get all the path from the departure airport to the arrival airport with the network. The possible paths are calculated one by one, considering the objective function, contrail size by inputting into the aircraft performance model and contrail length calculation. The new result is compared with the best-known solution from previous iterations until the allowed calculation time ends. To limit the aircraft from changing its altitude too many times, simplifying the resulted flight path, a limit is set to the allowed number of altitude changes, which can be user defined. The more the allowed number of altitude changes, the more the possible flight path. The last best-known result from all the iteration calculated would be the final result to the optimization problem, creating the flight path by showing the waypoint and flight altitude passed through.

3.6.4. Contrail Size Calculation

The optimization in the previous sections would only estimate the contrail length of the flight, which is the traveling distance in contrail formation area. This part of the program would estimate the contrail size by using the coordinate and flight information from the optimized path, for further investigation in effectiveness.

As this paper only concern the cruising stage of the flight, only contrail created at and affect by the cruising

stage, only the contrail size at cruising and descending for approach is considered. Through simple trigonometry, the amount of contrail is determined within a fixed dimension. Multiplying the contrail amount to the size of the grid, the contrail area size can be determined for the optimized path.

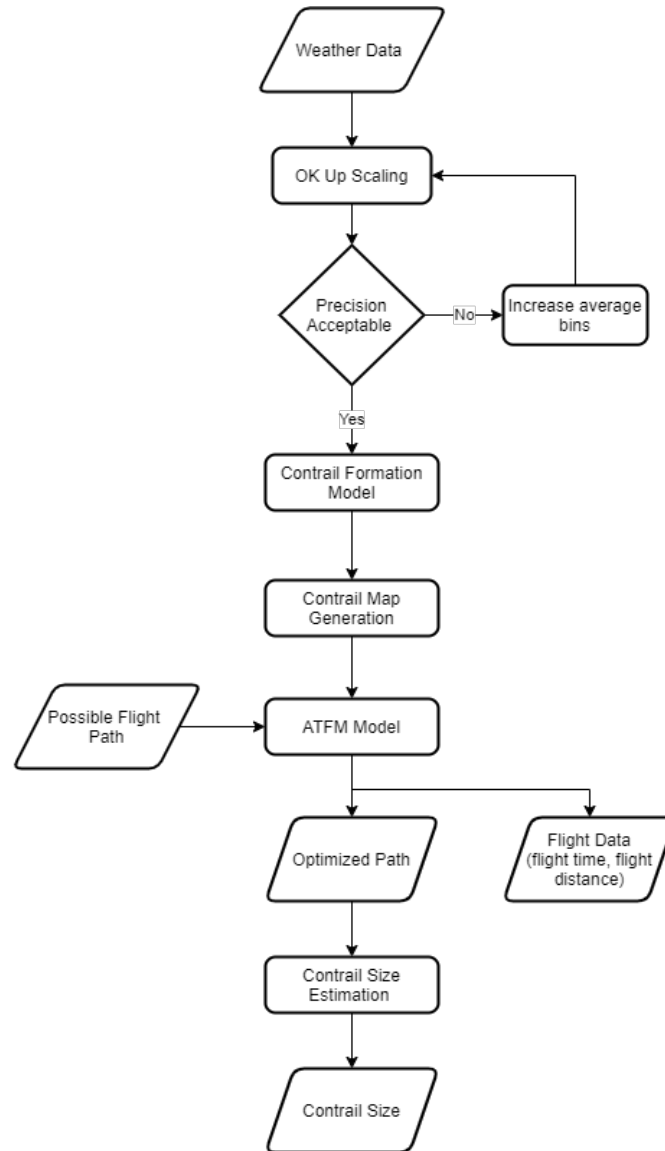


Figure 15: Flow Chart of Program

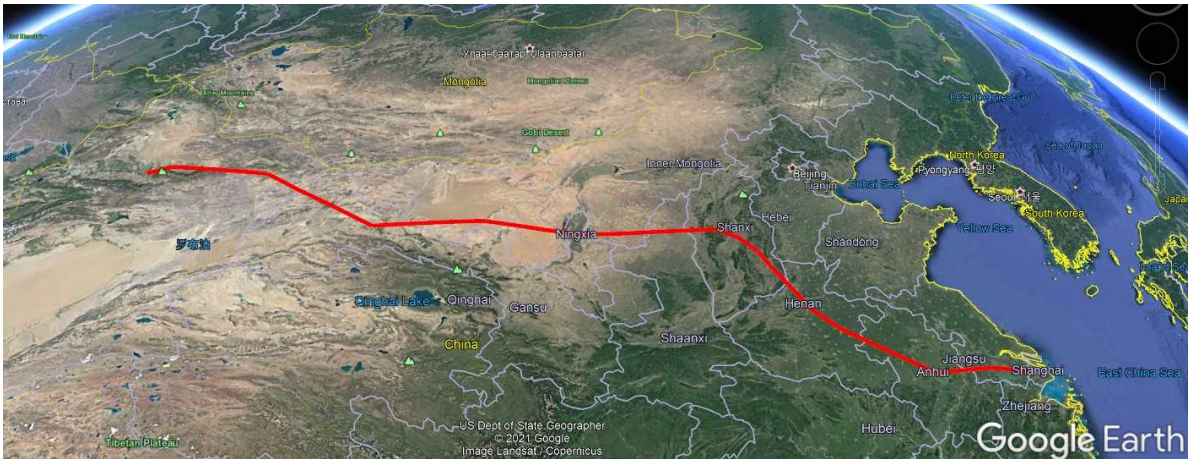
4. Discussion

4.1. Case study

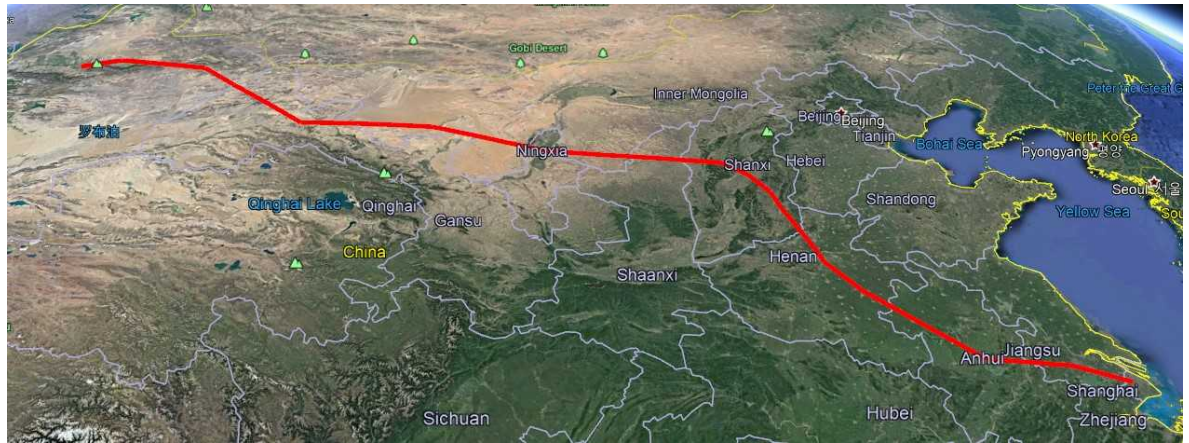
To study the effects of the contrail control programme, we will be using a real-life flight route for studying. The route we will be using is the China Southern Airlines flight 6981, from Urumqi Diwopu International Airport to Shanghai Hongqiao International Airport. This is a daily flight typically serviced by B787-8 and B737-800 aircrafts.

4.1.1. Flight path

1 As the wind state and traffic are different every day, the flight path would have some deviation. For example,
2 the flight would use different standard instrument departure (SID) under different wind direction when take-off,
3 affecting its later flight path. Through investigating on the flight path of different days on flightrader24 and
4 flightaware, it is concluded that 6 flight paths are more commonly used. This case study considered these 6
5 paths as optimization option while ignoring other possible paths that are rarely used or unused. During
6 calculation, we will limit the amount of flight level change allowed for the aircraft between 2 to 4 changes per
7 flight. While our main objective is to study the possibility for contrail size reduction, we will also calculate the
8 possible solutions for reduced flight time and compare the results with the solution of reducing contrail size.
9



10
11 **Figure 16. Alternative track 1.**



13
14 **Figure 17. Alternative track2.**

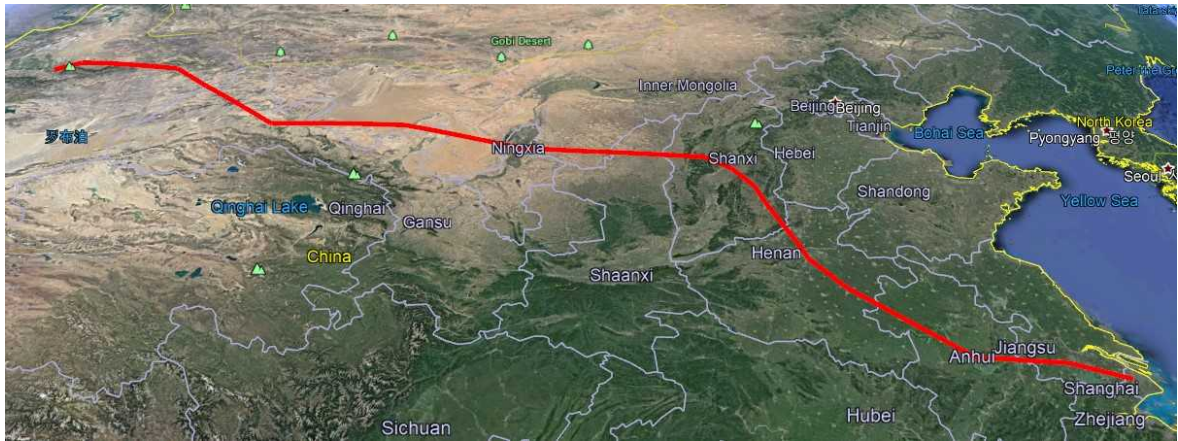


Figure 18. Alternative track 3.

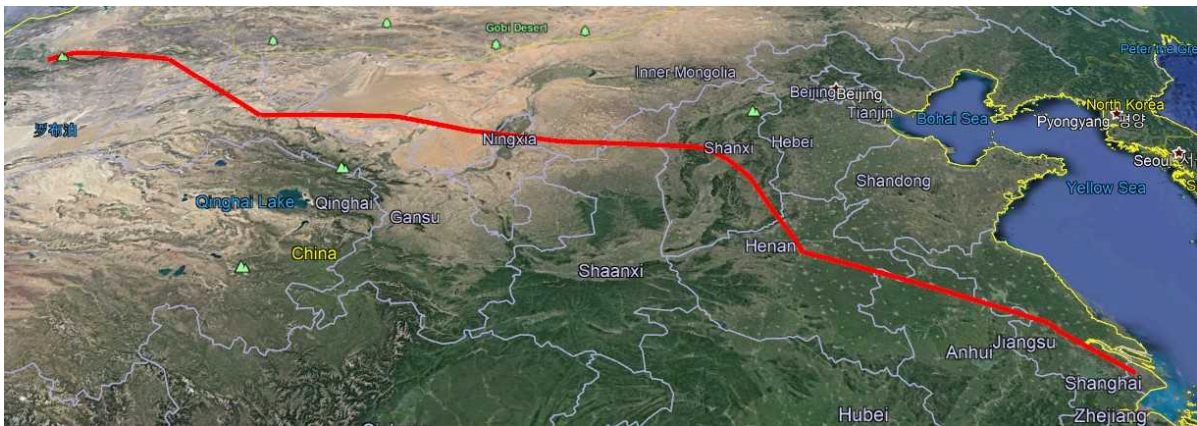


Figure 19. Alternative track 4.



Figure 20. Alternative track 5.

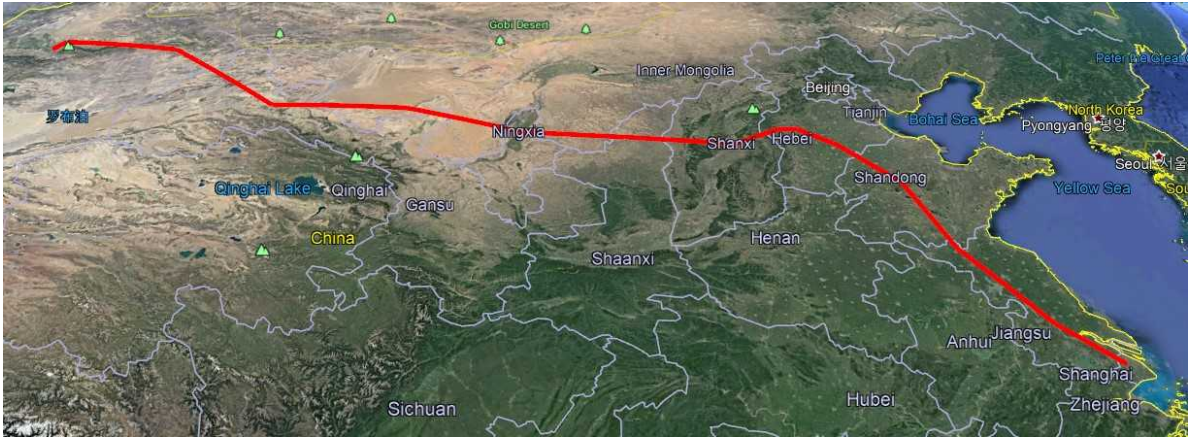


Figure 21. Alternative track 6.

4.1.2. Parameter settings

Parameters involved in determining the optimum flight path are described below. Real life weather data will be used to assess the operating environment along the flight path of the aircraft. To match the typical cruising altitude of the aircraft, we will only be considering data from 35000 feet upwards to 41000 feet. The aircraft is only allowed to choose 1 out of 6 alternative routes, with flight level changes only permitted when it arrives on a pre-determined waypoint. We will also only consider B787-8 as the route is served by B787-8 for most of the duration.

4.1.3. Time Period

For the case study, we will only be considering the data collected within a single week. This is because the programme is intended for short term use, and a new solution should be generated at the start of each flight. In addition, by considering a shorter time frame, the data will be more accurate with less deviation, allowing us to generate a better flight path. Moreover, by just considering the weather data from a single week, we can save on computing resources.

4.1.4. Map Scaling and Resolution

The map for the path optimization will be scaled at 765 pixels \times 560 pixels. There are several reasons for capping the resolution at this size. First, there is limitation in the instrumentation that is used to run the programme. For extremely high resolution on mapping, the time required is not efficient for the initial objective, which is optimization of flight path. As such, the prolonged time is not favourable in practical use, given that flight plans are usually obtained just hours before the actual flight. In addition, the limited number of weather station and way points along the flight path can provide limited resolution of weather data as well as path optimization for the optimization purpose. Therefore, even if the map is scaled at higher resolution, the enhancement in optimization performance is not proportional to the extra time cost. On the contrary, the resolution cannot be too coarse that the optimization performance will be hindered and barely meet the optimization purpose.

4.2. Case Study Result

For the case study, we have complied 10 separate flight routes for 3 different cases, in accordance with the number of flight level changes allowed. There are also 6 different set of waypoints for the aircraft to choose from.

Table 3

For a maximum of 2 flight level changes

	Flight time (secs)	Distance (Nautical Miles)	Contrail size (Square meter)
01-Jan 0000	15,734	101.9766	26,648,179
01-Jan 1200	15,733	101.9712	27,869,872
02-Jan 0000	15,734	101.9781	10,995,237
02-Jan 1200	15,739	101.964	27,869,872
03-Jan 0000	15,734	101.9643	27,869,872
03-Jan 1200	15,735	101.9728	23,212,167
04-Jan 0000	15,736	101.9876	1,145,337
04-Jan 1200	15,738	101.972	5,039,484
05-Jan 0000	15,739	101.9753	0
05-Jan 1200	15,736	101.9626	10,842,525

Table 4

For a maximum of 3 flight level changes

	Flight time (secs)	Distance (Nautical Miles)	Contrail size (Square meter)
01-Jan 0000	15,740	101.9963	26,648,179
01-Jan 1200	15,736	101.9687	27,869,872
02-Jan 0000	15,739	101.9792	10,995,237
02-Jan 1200	15,733	101.9613	27,869,872
03-Jan 0000	15,736	101.9661	27,869,872
03-Jan 1200	15,735	101.9645	23,212,167
04-Jan 0000	15,738	101.9942	1,145,337
04-Jan 1200	15,736	101.9683	5,039,484
05-Jan 0000	15,736	101.9784	0
05-Jan 1200	15,736	101.9711	10,842,525

Table 5

For a maximum of 4 flight level changes

	Flight time (secs)	Distance (Nautical Miles)	Contrail size (Square meter)
01-Jan 0000	15,736	101.9766	26,648,179
01-Jan 1200	15,739	101.9804	27,869,872
02-Jan 0000	15,739	101.9757	10,995,237
02-Jan 1200	15,738	101.9994	27,869,872
03-Jan 0000	15,736	101.9882	27,869,872
03-Jan 1200	15,733	101.9764	23,212,167
04-Jan 0000	15,735	101.9771	1,145,337
04-Jan 1200	15,736	101.9838	5,039,484
05-Jan 0000	15,740	101.9868	0
05-Jan 1200	15,738	101.9724	10,842,525

4.2.1. Result Analysis

From the above case study result, we can observe that the programme was able to generate a flight path in accordance with the equations discussed in section 2 and 3; however, the final solutions generated for all 3 scenarios are similar.

The flight time for the 10 different flight paths is close to each other, which is around 4 hours, with a small difference of a few seconds. The programme was able to compare the flight time and contrail size of the different solutions and come up with the best flight path. Using the result of 1st of January 00:00 as an example, in the case for 4 allowable flight level changes, the final solution flight time of 15736 seconds was the lowest out of the 1100 iterations, which is around 30 seconds faster than that of the highest calculated flight time.

The total distance travelled by the aircraft is also similar, mostly in the range of 102 nautical miles. The minor difference in distance travelled could be due to different selections of waypoints or flight level changes in flight. For the contrail size, the results are similar in all 3 scenarios for the same set of data. Taking the results in 2nd of January as an example, it is observed that contrail size estimated are all the same throughout the 3 scenarios, despite having different number of flight level changes allowed. This phenomenon persisted across the data of all 5 days for several reasons. First is the inaccuracy of the weather data available. Along the flight path and in certain flight level, some of the data is missing either due to lack of monitoring in the area or censorship. This created instances where the weather in a certain waypoint has to be estimated by using data collected from nearby weather stations and with the use interpolation method. This will affect the result of the programme as the weather data calculated will have discrepancies when comparing to the reality. This is most common near the western region in China, such as near Urumqi and areas with low population, as those areas tend to have lower weather stations density and weather balloons. Moreover, the locations in which the case study flight will pass through are also not ideal. The Urumqi to Shanghai flight mostly travelled in the northern region of China, where local climate is more favourable to the formation of contrails. This resulted in the aircraft constantly

1 flying in contrail formation zone, which hindered the effectiveness and significance of our programme.
2
3 From figures below, in the case on January 2nd, the programme was able to generate the most optimum flight
4 path for the aircraft to take, including changing the flight level of the aircraft. While the contrail forming
5 possibility is the same throughout the 6 possible flight paths, we are able to recommend a different solution to
6 the aircraft based on the number of allowed flight level changes. This suggests that the programme executed
7 intended function as expected. While the flight level changes were recorded, most of them happened during the
8 flight between waypoints. And as we had set the requirement for the aircraft to only change its altitude when
9 arriving at a waypoint and entering a contrail formation zone, these climbs and descends recommendations were
10 ignored, leading to very little change in the final en-route altitude of the aircraft.

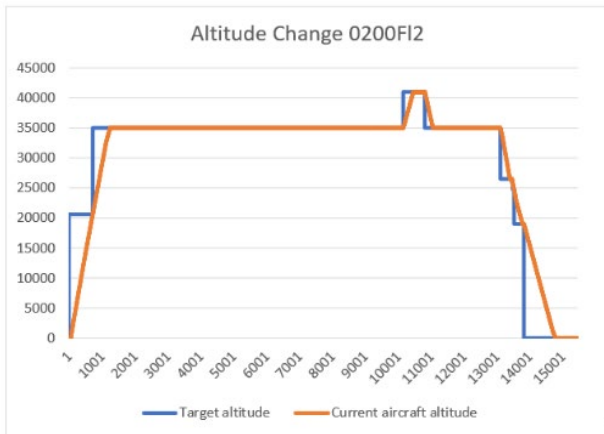


Figure 22. Change in altitude for case Jan 2nd @ 00:00, allowable level change = 2.

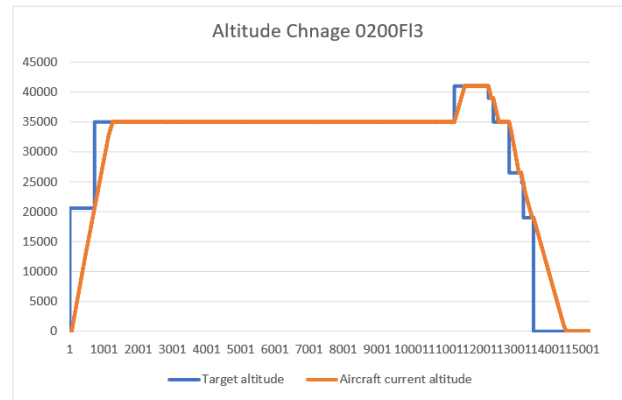


Figure 23. Change in altitude for case Jan 02 @00:00, allowable level change = 3.

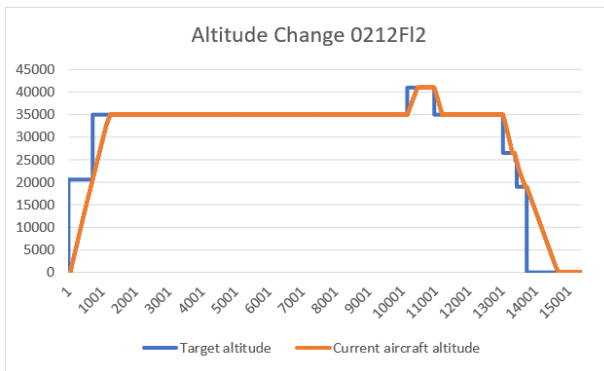


Figure 24. Change in altitude for case Jan 2nd@12:00, allowable level change = 2.

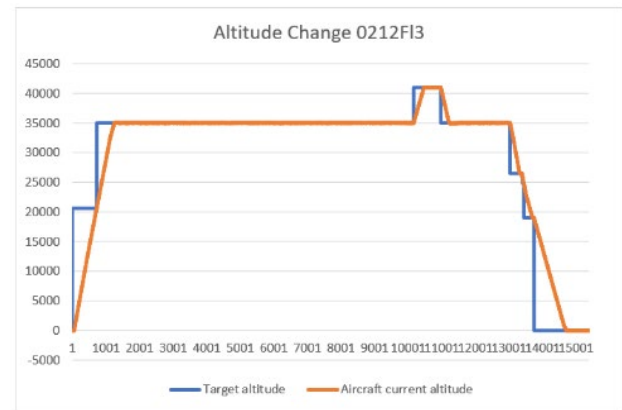


Figure 25. Change in altitude for case Jan 02 @12:00, allowable level change = 3.

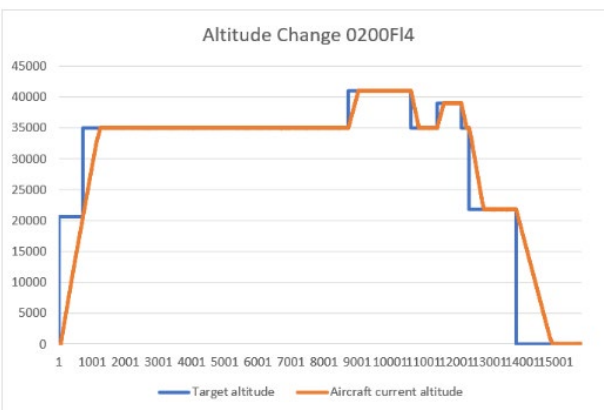


Figure 26. Change in altitude for case Jan 02 @00:00, allowable level change = 4.

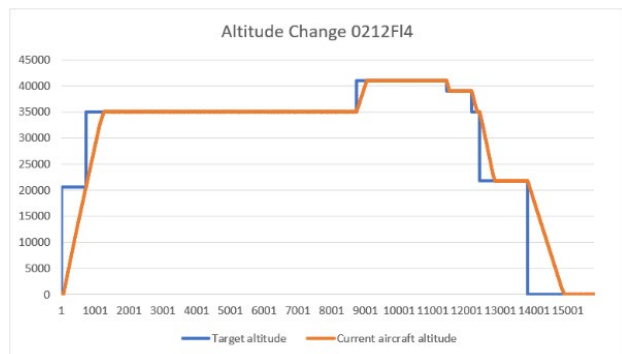


Figure 27. Change in altitude for case Jan 02 @12:00, allowable level change = 4.

5. Conclusion

In this project, the literature concerning the cause and impact of contrail formation has been researched, where the issue was addressed and the measures to mitigate the phenomenon are considered. Therefore, more research on existing models that provides the platform for simulation of the actual situation has been done, in order to meet the objective of minimizing formation of contrail in a flight through changing its flight path. For the realistic purpose and the practical use, it was attempted to connect the reality with simulation by integrating actual flight waypoints and genuine weather data into the simulation. There has been attempts to seek for an optimized flight path, but a conclusion cannot be completely drawn, and the results are not significant as intended due to the following limitations.

The flight profile is presented in a 2D manner by changing flight levels only, which in reality the aircraft can have the extra options of manoeuvring to right or left to avoid formation of contrail. Also, as the project is single objective oriented, which only focuses on flight path optimization with respect to mitigate contrail formation and to minimize its environmental impact, other potential influence on the environment, such as the extra greenhouse gases that may result by excess fuel burn due to optimization of flight path are not taken into account. Another limitation would be the limited number of waypoints and weather stations along the flight path. As flights usually follows a series of waypoints along their flight path in reality, the waypoints fixated the resolution of the map as the aircrafts must pass through them during the flight. On the other hand, as weather stations are not available all along the flight path, the weather condition on the flight path has to be estimated using interpolation methods, which may have discrepancy with the actual situation and affect the accuracy of calculation as well as flight path optimization performance adversely. In our case study, most samples show very constant flight trajectories with only very minimal change or even no change in flight levels. This is because the aircraft in the simulation need to satisfy both conditions of entering a contrail zone and reaching a waypoint to result a change in flight level and optimize the flight path. As the programme runs with smaller number of waypoints than the reality, it is more difficult to satisfy both above conditions in simulation.

In the future, more case studies can also be carried out for different flights, including those flying across different continents or flying from north to south or south to north, which could have greater difference in terms of weather and climate and the possibility for changes in flight level for optimization throughout the flight could be more significant. Tthe border between contrail zone and non-contrail zone crosses from west to east, which is the direction of the case study's flight. Flight paths with higher availability of weather data could also be chosen to minimize the discrepancy caused by interpolation estimates. In addition, instrumentation of higher performance specification could be used to obtain results of higher resolution or accuracy, as we have set limited waypoints in the simulation for this project due to instrumentation limitations. Furthermore, 3D or 4D flight path optimization could be used to provide more options for flight trajectory optimization.

Uncategorized References

- [1] B. Owen, D. S. Lee, and L. Lim, "Flying into the future: aviation emissions scenarios to 2050," ed: ACS Publications, 2010.
- [2] U. Burkhardt and B. Kärcher, "Global radiative forcing from contrail cirrus," *Nature climate change*, vol. 1, no. 1, pp. 54-58, 2011.
- [3] IATA, "Number of flights performed by the global airline industry from 2004 to 2021 (in millions)," ed: Statista, 2020.
- [4] P. M. Kuhn, "Airborne observations of contrail effects on the thermal radiation budget," *Journal of the Atmospheric Sciences*, vol. 27, no. 6, pp. 937-942, 1970.
- [5] R. R. Friedl, "Atmospheric effects of subsonic aircraft: Interim assessment report of the advanced subsonic technology program," 1997.
- [6] U. Schumann, "The impact of nitrogen oxides emissions from aircraft upon the atmosphere at flight altitudes—Results from the AERONOX project," *Atmospheric Environment*, vol. 31, no. 12, pp. 1723-1733, 1997.
- [7] D. S. Lee *et al.*, "Aviation and global climate change in the 21st century," *Atmospheric Environment*, vol. 43, no. 22-23, pp. 3520-3537, 2009.
- [8] T. Koop, B. Luo, A. Tsias, and T. Peter, "Water activity as the determinant for homogeneous ice nucleation in aqueous solutions," *Nature*, vol. 406, no. 6796, pp. 611-614, 2000.
- [9] A. Bier and U. Burkhardt, "Variability in contrail ice nucleation and its dependence on soot number emissions," *Journal of Geophysical Research: Atmospheres*, vol. 124, no. 6, pp. 3384-3400, 2019.
- [10] R. H. Moore *et al.*, "Biofuel blending reduces particle emissions from aircraft engines at cruise conditions," *Nature*, vol. 543, no. 7645, pp. 411-415, 2017.
- [11] UNFCCC, "Fact sheet: Climate change science—the status of climate change science today," in *United Nations Framework Convention on Climate Change*, 2011.
- [12] U. S. G. C. R. Program, "Climate Science Special Report: Fourth National CLimate Assessment," vol. I, 2017.
- [13] T. I. P. o. C. Change, "WG1AR5 Annex III," 2013.
- [14] K. Hansen, "Water Vapor Confirmed as Major Player in Climate Change," 2008. [Online]. Available: https://www.nasa.gov/topics/earth/features/vapor_warming.html.
- [15] G. A. Schmidt, R. A. Ruedy, R. L. Miller, and A. A. Lacis, "Attribution of the present-day total greenhouse effect," *Journal of Geophysical Research: Atmospheres*, vol. 115, no. D20, 2010.
- [16] T. I. P. o. C. Change, "AR5 Synthesis Report: Climate Change 2014," 2014. [Online]. Available: <https://www.ipcc.ch/report/ar5/syr/>.
- [17] ICAO, "Aircraft Engines Emission," n.d. [Online]. Available: <https://www.icao.int/environmental-protection/pages/aircraft-engine-emissions.aspx>.
- [18] D. Lee *et al.*, "The contribution of global aviation to anthropogenic climate forcing for 2000 to 2018," *Atmospheric Environment*, vol. 244, p. 117834, 2020.
- [19] NASA, "Chemistry of Ozone Formation," 2003. [Online]. Available: https://earthobservatory.nasa.gov/features/ChemistrySunlight/chemistry_sunlight3.php.
- [20] C. Frömming, M. Ponater, K. Dahlmann, V. Grewe, D. Lee, and R. Sausen, "Aviation-induced radiative forcing and surface temperature change in dependency of the emission altitude," *Journal of Geophysical Research: Atmospheres*, vol. 117, no. D19, 2012.
- [21] A. G. Detwiler and A. Jackson, "Contrail formation and propulsion efficiency," *Journal of aircraft*, vol. 39, no. 4, pp. 638-644, 2002.
- [22] K. Gierens, B. Kärcher, H. Mannstein, and B. Mayer, "Aerodynamic contrails: Phenomenology and flow physics," *Journal of the atmospheric sciences*, vol. 66, no. 2, pp. 217-226, 2009.
- [23] H. Appleman, "The formation of exhaust condensation trails by jet aircraft," *Bulletin of the American Meteorological Society*, vol. 34, no. 1, pp. 14-20, 1953.
- [24] O. Von Stryk and R. Bulirsch, "Direct and indirect methods for trajectory optimization," *Annals of operations research*, vol. 37, no. 1, pp. 357-373, 1992.
- [25] K. K. H. Ng, C.-H. Chen, and C. K. M. Lee, "Mathematical programming formulations for robust airside terminal traffic flow optimisation problem," *Computers & Industrial Engineering*, vol. 154, p. 107119, 2021, doi: <https://doi.org/10.1016/j.cie.2021.107119>.
- [26] E. T. Turgut and M. A. Rosen, "Relationship between fuel consumption and altitude for commercial aircraft during descent: preliminary assessment with a genetic algorithm," *Aerospace Science and Technology*, vol. 17, no. 1, pp. 65-73, 2012.
- [27] B. D. Dancila and R. M. Botez, "Vertical flight path segments sets for aircraft flight plan prediction and optimisation," *The Aeronautical Journal*, vol. 122, no. 1255, pp. 1371-1424, 2018.
- [28] N. K. Wickramasinghe, A. Harada, and Y. Miyazawa, "Flight trajectory optimization for an efficient air transportation system," in *28th International Congress of the Aeronautical Science (ICAS 2012)*, 2012.
- [29] A. Gardi, R. Sabatini, and T. Kistan, "Multiobjective 4D trajectory optimization for integrated avionics and air

- traffic management systems," *IEEE Transactions on Aerospace and Electronic Systems*, vol. 55, no. 1, pp. 170-181,2018.
- [30] B. Dancila, R. Botez, and D. Labour, "Altitude optimization algorithm for cruise, constant speed and level flight segments," in *AIAA guidance, navigation, and control conference*, 2012, p. 4772.
- [31] A. Murrieta Mendoza, "Vertical and lateral flight optimization algorithm and missed approach cost calculation," École de technologie supérieure, 2013.
- [32] N. Dougui, D. Delahaye, S. Puechmorel, and M. Mongeau, "A light-propagation model for aircraft trajectory planning," *Journal of Global Optimization*, vol. 56, no. 3, pp. 873-895,2013.
- [33] D. González-Arribas, M. Soler, and M. Sanjurjo-Rivo, "Robust aircraft trajectory planning under wind uncertainty using optimal control," *Journal of Guidance, Control, and Dynamics*, vol. 41, no. 3, pp. 673-688,2018.
- [34] A. Murrieta-Mendoza, C. Romain, and R. M. Botez, "3D cruise trajectory optimization inspired by a shortest path algorithm," *Aerospace*, vol. 7, no. 7, p. 99,2020.
- [35] G. Serafino, "Multi-objective aircraft trajectory optimization for weather avoidance and emissions reduction," in *International Workshop on Modelling and Simulation for Autonomous Systems*, 2015: Springer, pp. 226-239.
- [36] J. Rosenow and H. Fricke, "Individual condensation trails in aircraft trajectory optimization," *Sustainability*, vol. 11, no. 21, p. 6082,2019.
- [37] F. Yin, V. Grewe, C. Frömming, and H. Yamashita, "Impact on flight trajectory characteristics when avoiding the formation of persistent contrails for transatlantic flights," *Transportation research part D: Transport and environment*, vol. 65, pp. 466-484,2018.
- [38] R. S. Félix Patrón and R. M. Botez, "Flight trajectory optimization through genetic algorithms coupling vertical and lateral profiles," in *ASME international mechanical engineering congress and exposition*, 2014, vol. 46421: American Society of Mechanical Engineers, p. V001T01A048.
- [39] V. Klein and K. D. Noderer, "Modeling of aircraft unsteady aerodynamic characteristics. Part 1: Postulated models," 1994.
- [40] A. Nuic, C. Poinso, M.-G. Iagaru, E. Gallo, F. A. Navarro, and C. Querejeta, "Advanced aircraft performance modeling for ATM: Enhancements to the BADA model," in *24th Digital Avionics System Conference*, 2005: AIAA/IEEE Washington, DC, pp. 1-14.
- [41] J. Sun, J. M. Hoekstra, and J. Ellerbroek, "OpenAP: An open-source aircraft performance model for air transportation studies and simulations," *Aerospace*, vol. 7, no. 8, p. 104,2020.
- [42] J.-P. Chilès and N. Desassis, "Fifty years of kriging," in *Handbook of mathematical geosciences*: Springer, Cham, 2018, pp. 589-612.
- [43] J. Sun, J. Ellerbroek, and J. M. Hoekstra, "WRAP: An open-source kinematic aircraft performance model," *Transportation Research Part C: Emerging Technologies*, vol. 98, pp. 118-138,2019.